E-20 - K04
#8

EVALUATION OF THE PERFORMANCE OF STEEL PEDESTALS UNDER LOW SEISMIC LOADS

GDOT-RP2048
Report No. 9
Final Report

Submitted by: M. Hite, R. DesRoches, R. Leon
Georgia Institute of Technology

TABLE OF CONTENTS

I. RECOMMENDATIONS FOR BRIDGE STEEL PEDESTALS

A. SCOPE

The recommendations for bridge steel pedestals are based on a series of six full-scale reversed cyclic quasi-static experimental tests that were conducted on a two-girder 40' simply-supported bridge span at the Structures Laboratory at the Georgia Institute of Technology (Figure 1). A summary of the test results and analyses are presented in the Appendices of this report. In assessing the performance of bridge steel pedestals, both experimentally and analytically, three critical factors were identified and are recommended as best practices and design guidelines for the performance of bridge steel pedestals.

NOTE: The effect of bridge skew and horizontal curvature is beyond the scope of this research in providing recommendations. However, it is understood that transverse movement may become significant for skew angles greater than 20° in which the bearings are not aligned parallel to the movement of the structure, where designers shall abide by the appropriate requirements and codes for quality bridge performance.

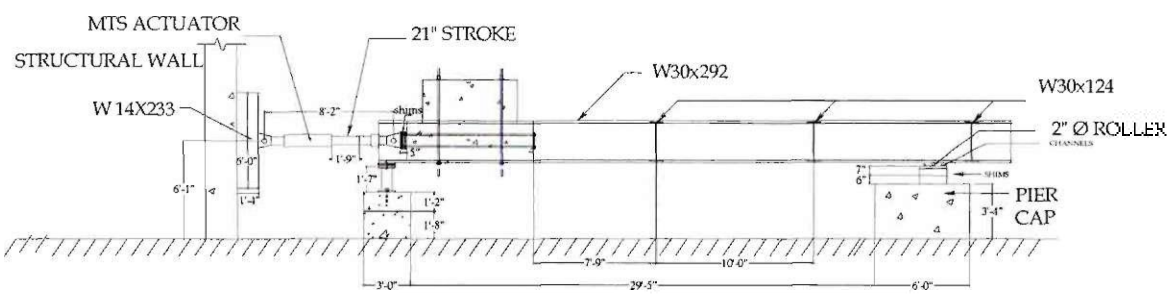

Figure 1: Experimental test setup of 40' bridge specimen rehabilitated with short-19" pedestals

B. BEST PRACTICES FOR BRIDGE STEEL PEDESTALS

1. Construction tolerances to reduce effect of loading eccentricities

Best practice #1: *The centerlines of the girders shall be properly aligned within 0.25" of the centerlines of steel pedestals to minimize the effect of loading eccentricities.*

Reference: AASHTO LRFD Bridge Design Specifications, Article 2.5.3 "Constructability"[1]

Construction misalignments often contribute to loading eccentricities. Loading eccentricities may result in limiting the ultimate strength and deformation of the system and may cause a mechanism leading to a mode of failure. Therefore, it is imperative that the centerlines of the girders and steel pedestals are properly aligned and level. Axial compression tests of the steel pedestals were conducted to study the effect of loading eccentricities, which showed the importance of proper alignment as the pedestals were sensitive to very slight eccentricities[2]. A recommended construction tolerance of less than 0.25" is suggested to minimize critical eccentricities over the web and at the centerlines. According to AASHTO LRFD Article 2.5.3, "Bridges should be designed in a manner such that fabrication and erection can be performed without undue difficulty or distress and that locked-in construction force effects are within tolerable limits."

[1] AASHTO LFRD Bridge Design Specifications, 2004. Section 2: General Design and Location Features.
[2] GDOT RP2048, Report No. 7, January-March, 2006.

2. Minimum concrete edge distance

Best practice #2: *The minimum concrete edge distance shall be taken as $6d_o$, where d_o is the bolt diameter at the concrete surface.*

Reference: ACI 318-05, Appendix D, Code D.8.3[3]

Minimum concrete edge distance is critical in the placement of the post-installed stud anchor bolts to fully develop the capacity of the bolts and minimize the concrete damage. Concrete breakout occurs when the concrete fractures before the load-carrying capacity of the steel is reached. For test P2-1, the tall pedestal was loaded along the plane of its strong-axis, where weld fracture occurred due to flexural bending of the weld during cyclic loading. The concrete breakout essentially consisted of unconfined concrete as a result of the anchor bolt being close to the edge of the concrete pier. The surface failure occurred at the predicted angle of 35° as shown in Figure 2. Past studies have shown anchor bolts to result in concrete damage during seismic loading similar to the concrete breakout that was observed in test P2-1. (More details of test P2-1 can be found in the *Testing of Bridge Steel Pedestals* section of the Appendices). In cases where the specified minimum concrete edge distance is not satisfied, measures shall be taken to provide additional reinforcement. For instance, the reinforced concrete bent cap could be wrapped with fiber-reinforced polymers (FRP) or steel plates could be attached to provide confinement of the concrete.

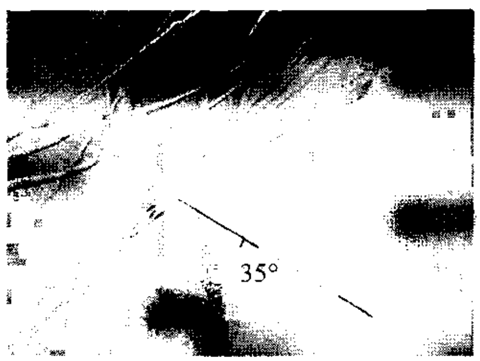

Figure 2: Concrete breakout at 35° on concrete pier due to insufficient concrete edge distance of the bolts

3. Minimum seat width

Best practice #3: *The minimum seat width shall be established based on the following:*

$$N = \left[100 + 1.7L + 7.0H + 50\sqrt{1 + (2\frac{B}{L})^2}\right]\left(\frac{1 + 1.25F_v S_1}{\cos\alpha}\right),$$

where N is in mm, L, B, and H are in meters and α is in degrees.

Reference: AASHTO, NCHRP 12-49 provisions, and FHWA/MCEER *Seismic Retrofitting Workshop Manual for Highway Structures: Part 1-Bridges*[4]

[3] American Concrete Institute (ACI), Reported by ACI Committee 318, 2005.

[4] U.S. DOT Federal Highway Administration and MCEER, Workshop at the 5th National Seismic Conferences on Bridges and Highways, San Mateo, California, September 2006.

The determination of minimum seat width is critical since the steel pedestals may undergo considerable movement due to kinematic motion during cyclic loading, where both sliding and rocking occur on the abutment seat (see the *Testing of Bridge Steel Pedestals* section of the Appendices for more details). The minimum seat width shall be established to avoid unseating of the bridge deck. Since the prediction of relative movement is often difficult to determine, the minimum support length can be calculated by:

$$N = \left[100 + 1.7L + 7.0H + 50\sqrt{1 + (2\frac{B}{L})^2} \right] (\frac{1 + 1.25F_v S_1}{\cos\alpha})$$

where the FHWA/MCEER *Seismic Retrofitting Workshop Manual for Highway Structures: Part 1-Bridges* defines the input variables as follows:

- N is the recommended support length measured from the normal to the face of an abutment or pier (mm)
- L is the length of the bridge deck from the seat to the adjacent expansion joint, or to the end of the bridge deck (m). For hinges or expansion joints within a span, L is the sum of the distances on either side of the hinge (m); for single-span bridges, L is the length of the bridge deck (m)
- H is the height. For abutment seats, H is the average height of piers or columns supporting the bridge deck between the abutment and the next expansion joint (m). For pier seats, H is the height of the pier (m); for hinge seats within a span, H is the average height of the two adjacent piers (m); for single-span bridges, H=0.
- B is the width of the deck (m); NOTE: the ratio B/L shall not be greater than 3/8
- α is the angle of skew (0° for a right bridge)
- $S_{D1} = F_V S_1$ is the product of the long-period soil factor (F_V) and the 1.0 second spectral acceleration (S_1)

In cases where the specified minimum seat width is not satisfied, measures shall be taken to provide additional seat width. Seat extensions could be used to provide additional seat width. The extensions shall be anchored to the vertical face of the concrete abutment or pier with dowels or anchor bolts. These dowels or anchor bolts shall be designed to carry large vertical and horizontal forces due to the loads imposed by the superstructure if the bearings were to fail. Post-tensioning the seat extensions to the substructure is recommended when feasible.[4]

C. Design Guidelines for Bridge Steel Pedestals

1. Stud anchor bolt design strength

Guideline #1: The swedged stainless steel stud anchor bolts shall be covered with a minimum of Grade 36, thereby providing a minimum yield strength of 36 ksi instead of 30 ksi as indicated by the manufacturer's readings for the swedged stainless steel stud anchor bolts used in the experimental testing.

Reference: Steel Anchor Bolts AASHTO Designation: M 314-90 (1996)[5]

The stud anchor bolts connected to the steel pedestals shall consist of swedged stainless steel and conform to the standard specifications for steel anchor bolts as prescribed in the AASHTO Designation M 314-90. The mechanical properties of the swedged stainless steel post-installed stud anchor bolts from the manufacturer[6] used for the experimental investigation are shown in Table 1. However, based on the AASHTO Designation M 314-90 Article 4, the anchor bolts shall be covered with a minimum of Grade 36, thereby providing a yield strength of 36 ksi instead of 30 ksi.

The steel pedestal stud anchor bolts shall be designed such that the anchor bolt resistance is "governed by a ductile steel element or the yield capacity of a ductile steel attachment to which the anchors are connected."[7] Forcing this mechanism ensures some measure of ductile response although the aforementioned guideline cannot be expected to be "earthquake proof."

Table 1: Stainless steel anchor bolts manufacturer's "Mill Test Analysis Certificate" readings 1/31/2006

[illegible]	YIELD STRENGTH (ksi)	TENSILE [illegible] (ksi)
Min	30	75
Results	57.6	92.8

2. Anchorage and grouting

Guideline #2: Stud anchor bolts shall be embedded a minimum of [12", $12d_b$], not to exceed 2/3 of the member thickness, and shall be anchored in a non-shrink grout that conforms to ASTM C1107 and the Corps of Engineers Specification: CRD-C 621.

Guideline #3: A minimum edge distance twice the maximum aggregate size shall be used as to not cause microcracking when drilling the holes for the post-installed stud anchor bolts.

Reference: ASTM C 1107, Grades A, B, and C; Core of Engineers Specification, and ACI Appendix D

Proper anchorage of the stud anchor bolts is important for the development of the bolt capacity. The stud anchor bolts shall be embedded no deeper than 2/3 of the member thickness and shall be anchored in a non-shrink grout that conforms to ASTM C 1107 and the Corps of Engineers Specification:

---

[5] Standard Specifications for Transportation Materials and Methods of Sampling and Testing, Part I – Specifications, American Association of State Highway and Transportation Officials (AASHTO), 2000.

[6] Atlanta Rod & Manufacturing c/o Highway Materials (Bill Craddock), Ping Tai Stainless Works, Mill Test Analysis Certificate, 8/2006, 404.766.8098 FAX, 404.7666.1650 PHONE.

[7] Eligenhausen, R., Mallee, R., and Silva, J. *Anchorage to Concrete Construction*, Ernst & Sohn, Berlin, 2006.

CRD-C 621. Two types of grout were used: 1) Horn non-corrosive, non-shrink grout provided by Highway Materials conforming to ASTM C 827 and CRD-C 621 and 2) 588 Precision Grout from W. R. Meadows conforming to ASTM C 1107, Grades A, B, and C and CRD-C 621. Tests P1-1 through P2-1 were conducted using the Horn grout and tests P2-2 through P3-1 used the 588 Precision Grout. Tests P2-2 and P3-1 revealed better performance of the grout. In fact, test P2-2 showed the highest peak displacement of ±3.5" (see Appendix A for more details). Therefore, grouts conforming to CRD-C 621 and ASTM C 1107, Grades A, B, and C are recommended as guidelines for the bridge steel pedestals.

From RD.8.3 in the Commentary of Appendix D (318-05), it is important to note that "drilling holes for the post-installed stud anchor bolts can cause microcracking. The requirement for a minimum edge distance twice the maximum aggregate size is to minimize the effects of such microcracking." Although microcracking was not observed during the experimental investigation, the possibility for this occurrence shall be duly noted. Also, from RD.8.5, "post-installed anchors should not be embedded deeper than 2/3 of the member thickness." Both of these guidelines should help with quality control and development of the bolt capacity.

3. Expected spectral accelerations and seismic design categories for Georgia

Guideline #4: Dade, Catoosa, Walker and Chattooga Counties shall also be considered as Seismic Design Category B in Section II of GDOT's *Bridge General* specification based on expected spectral accelerations for that region.

Reference: United States Geological Survey[8]

Based on the U. S. Geological Survey Probabilistic Hazard 3.10 software, Dade, Catoosa, Walker and Chattooga Counties in Georgia should also be included as Seismic Category B given the expected spectral accelerations for the earthquake return periods of 500 (475), 1000 (975) and 2500 (2475) years for the state of Georgia. Since the spectral accelerations for Dade, Catoosa, Walker and Chattooga Counties exceed that of the expected spectral accelerations for Bartow County which is considered a seismic category B, Section II of GDOT's *Bridge General* specification shall also consider these four counties as seismic category B as shown in Figure 3. Table 2 presents the expected spectral accelerations for these counties as well as Atlanta (Fulton County) and Cartersville (Bartow County) at a *0.1-second* period of vibration.

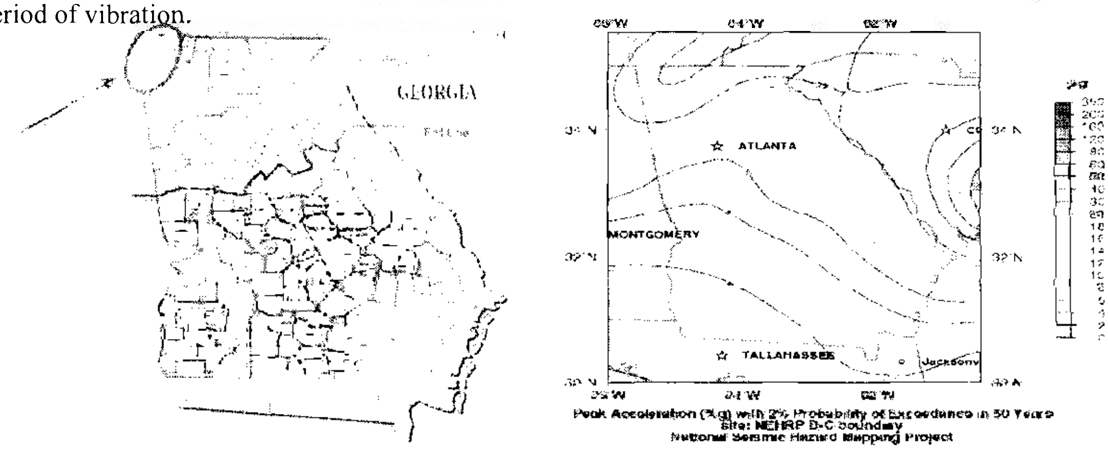

Figure 3: GDOT Section II-Bridge General Specification should also include Dade, Walker, Catoosa and Chattooga Counties in Seismic Category B (left) and 2500-year seismic hazard map (%g) for GA (2002)

[8] USGS (2006), *Seismic Hazard Curves and Uniform Hazard Response Spectra* Probabilistic Hazard 3.10 CD.

Table 2: Spectral accelerations (Sa) for return periods of 2500, 1000 and 500 years in GA at T_n = ***0.1 sec****

County in [illegible]	Sa (g)	1000_S[illegible]	500_S[illegible]
Catoosa	0.75	0.38	0.22
Walker	0.7	0.37	0.21
Dade	0.67	0.36	0.20
Chattooga	0.63	0.34	0.19
Bartow	0.45	0.22	0.14
Fulton	0.26	0.15	0.1

**Based on USGS Seismic Hazard Maps and Probabilistic Hazard 3.10 CD, 2006.*[6]

***Note:* Depending on the structural period, the spectral accelerations will vary; only the peak spectral accelerations are shown.**

D. BRIDGE VULNERABILITY ASSESSMENT

In addition to satisfying the best practices and design guidelines for bridge steel pedestals, a bridge vulnerability assessment needs to be conducted using the following step-by-step (10-step) procedure. Details for the analyses and an example problem specifically outlining the approach are described in the *Analyses of Bridge Steel Pedestals* section of the Appendices.

STEP

1. Idealize the bridge as a single-degree-of-freedom (SDOF) cantilever beam with a lumped mass representing the total mass of the bridge, M (Figure 4). The cantilever frame element now represents the summation of stiffness from all of the columns, $K_{columns}$.

2. Determine the number of pedestals on the bridge. Reference Table 3 and find the test series that corresponds with the height and loading orientation of the pedestals on the bridge. (See the *Testing of Bridge Steel Pedestals* section in the Appendices for more details).

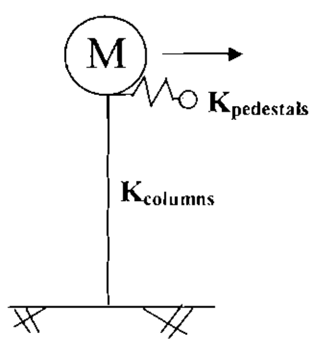

Figure 4: Idealization of bridge into a SDOF model of an upright cantilever beam with lumped mass

Table 3: Initial and peak effective stiffness values from force-displacement hysteretic relationships

Test: Pedest[illegible]	[illegible]	[illegible]eak Effective [illegible] of a Pedestal
P1-1: 19"	18.6	13.4
P1-2: 19"	17.9	13.5
P2-1: 33½"	20.5	12.1
P2-2: 33½"	27.1	8.27
P3-1: 33½"	20.4	24.8
P3-2: 33½"	24.8	13.7

3. Multiply the corresponding initial and peak effective stiffness values calculated from the force-displacement hysteretic behavior obtained from experimental testing by the number of pedestals. This yields the spring constant defined as a linear translational spring, which represents all of the pedestal stiffness, $K_{pedestals}$. The range of initial and peak stiffness are evaluated for each test to provide a range of structural periods.

4. Apply Equation 1 to determine the total stiffness, ΣK, of the idealized bridge structure.

5. Compute the natural frequency, ω_n, and structural period, T_n, using Equation 2 since the total mass and stiffness are known.

$$\sum K = \frac{K_{pedestals} K_{columns}}{K_{pedestals} + K_{columns}} \qquad \text{Eq. 1}$$

$$\omega_n = \frac{2\pi}{T_n} \quad \text{and} \quad T_n = 2\pi \sqrt{\frac{m}{\sum K}} \qquad \text{Eq. 2}$$

6. Generate the uniform hazard spectra using the *Probabilistic Hazard 3.10* software produced by Frankel, A. D. and Leyendecker, E. V. of the USGS. For example, the uniform hazard spectra (UHS) for Atlanta, Georgia given a 500 (10% PE in 50 years), 1000 (5% PE in 50 years) and 2500-year (2% PE in 50 years) return period earthquake is presented in Figure 5. The UHS for Cartersville (Bartow County) and Ringgold (Catoosa County) are also presented along with more details regarding UHS in the *Analyses of Bridge Steel Pedestals* section of the Appendices.

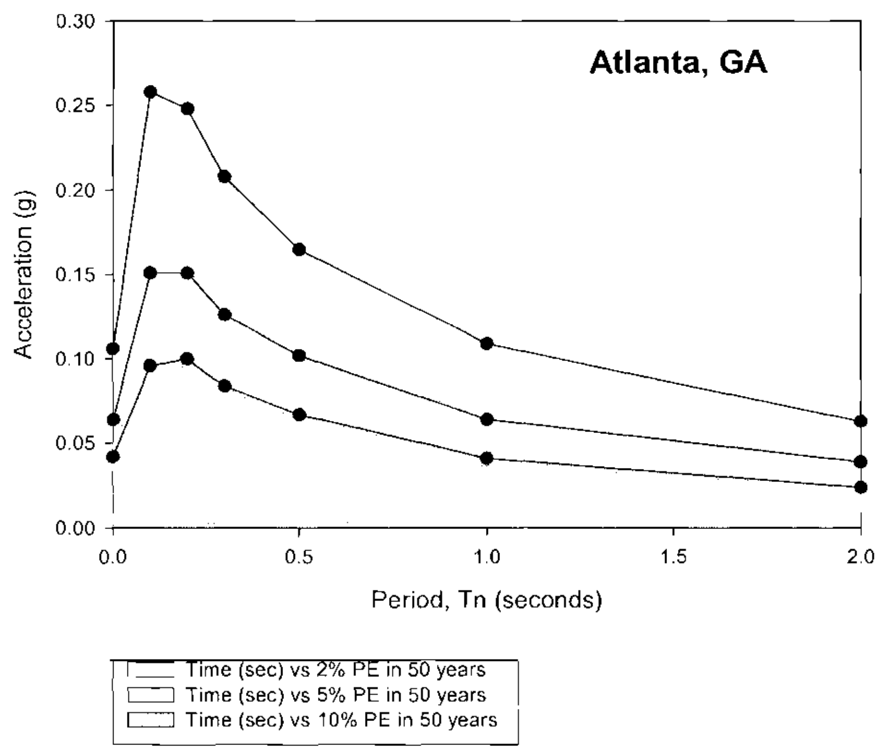

Figure 5: Uniform hazard spectra for Atlanta, GA for 2500, 1000, and 500-year return period EQ

7. Find the corresponding expected spectral acceleration for the structural period computed in Step 5.

8. Calculate the expected displacements from the spectral acceleration determined in Step 7 using Equation 3. The displacement demands are then compared to the peak displacements obtained from testing, which are deemed as the capacity of the steel pedestals.

$$D(inches) = \frac{A*(386)}{\omega_n^2}, \qquad \text{Eq. 3}$$

where A is the acceleration in units of g from the uniform hazard spectra.

9. Compute the demand to capacity ratio by dividing the displacement calculated in Equation 3 by the capacity achieved from the peak displacement obtained experimentally.

10. Evaluate the bridge vulnerability based on the demand to capacity ratio. A bridge is deemed to be "okay" if the demand to capacity ratio (D/C) is less than 1 (<1 is okay). If D/C > 1, a re-design of the pedestals shall be performed, considering the various pedestal types and configurations with their respective stiffness values.

D. Inspection and Maintenance

The steel pedestals should be inspected routinely to ensure that the ⅛" elastomeric (neoprene) pad has not "walked out" from under the steel pedestal and that the pedestals themselves are protected from corrosion. Based on AASHTO[3], "all exposed steel parts of bearings not made from stainless steel shall be protected against corrosion by zinc metallization, hot-dip galvanizing, or a paint system approved by the Engineer. Additionally, the steel pedestals should be carefully inspected for the presence of dirt or other debris that may prohibit movement of the pedestal. The use of stainless steel anchor bolts is the most reliable protection against corrosion because coatings of any sort are subject to damage by wear or mechanical impact." Therefore, a formally adopted, consistent maintenance inspection of the steel pedestals shall take place, where the elastomeric (neoprene) pad is inspected for proper seating and that the steel pedestals are protected from corrosion. Prioritization for inspection and maintenance can be based on the results from the bridge vulnerability discussed in the previous section. Table 4 shows a list of more than 50 bridges in Georgia that Bellamy Brothers (contractors) have elevated with steel pedestals.

Table 4: Bridges in Georgia that have been elevated with steel pedestals

COUNTY	BRIDGE NAME
Bibb-Monroe	Estes Rd Over I-475
"	Zebulon Rd Over I-475
"	I-475 Over Tobeso Pkee Creek
"	I-475 Over Tobeso Pkee Creek OverFlow
"	Eisenhower SR 80 Over I-475
"	SR 74 Mercer Rd Over I-475
"	SR 22 Clumbus Rd. Over I-475
"	I-475 over Rocky Creek
"	Peake Rd Over I-475
Bartow	Pleasant Valley Rd Over I -75
"	Cassville White Rd Over I - 75
Camden	St Mary's Rd Over I - 95

	Martin Luther King Over I - 95
	Harriett Bluff Over I - 95
Cherokee	Woodstock Rd Over I - 75
Cobb	Six Flags Rd Over I - 20
"	Factory Shoals Over I - 20
"	All Good Rd Over I - 75
"	Chastain Rd. Over I - 75
"	Hickory Grove Rd Over I - 75
"	Wade Green Rd Over I - 75
Crisp-Turner	Begood Rd Over I - 75
"	Hawpond Rd Over I - 75
"	Mussel White Rd Over I - 75
"	Old Hatley Rd. Over I - 75
"	Rock Wenona Rd. Over I - 75
"	Wardlow Rd Over I - 75
"	I - 75 Over
Dekalb	Fairington Rd Over I - 20
	Panthersville Rd Over I - 285
Fulton	Conley Rd. Over I -285
Henry	Locust Grove Rd. Over I - 25
"	Indian Creek Rd. Over I - 75
"	Bethlehem Rd. Over I - 75
Jackson	SR 82 Spur Over I - 85
"	SR 88 Over I - 85
"	Maysville Rd SR 98 over I - 85
"	SR 60 Over I - 85
Liberty	Isle of Wight Rd Over I-95
	SR 84 Over I-95
	Retreat Rd Over I-95
Lowndes	Shiloh Rd Over I-75
	SR 22 Over I-75
Peach-Hudson	SR 26 Over I - 75
"	Firetower Rd Over I - 75
"	Gaines Dr. Over I - 75
"	Todd Rd. Over I - 75
"	Thompson Rd Over I - 75
Richmond	Wheeler Rd Over I-520
"	Wrightsboro Rd over I-520
"	CSTX Crossing Over I-520
"	SR 278 Over I-520

"	Milledgeville Rd Over I-520
Tift	Chula Brookfield Rd Over I - 75
	Willis Stills Rd Over I - 75
	Bnghton Rd Over I-75
	Westley Rigdon Over I-75
Troup	Old West Point Over I-20

II. APPENDICES

A. Testing of Bridge Steel Pedestals

A1. Summary of experimental test results

Six full-scale, reversed cyclic quasi-static tests of a 40' bridge specimen rehabilitated with steel pedestals were conducted to assess the capacity of the steel pedestals. Two tests were conducted with the 19" (short) pedestals (Figure A1) and four tests were conducted with the 33½" (tall) pedestals (Figure A2). Various configurations of the anchor bolts and direction of loading on the pedestal cross-sections were tested to determine the effect on the performance of the steel pedestals. The force-displacement plots show the inelastic behavior of the pedestals when subjected to cyclic loading. The force-displacement plots also provide a basis for assessing the capacity of the steel pedestals in terms of peak loads and displacements.

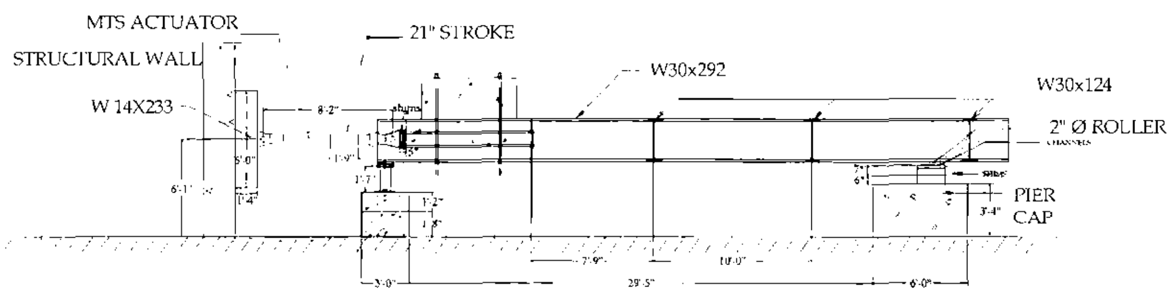

Figure A1: Experimental test setup of 40' bridge specimen rehabilitated with short-19" pedestals

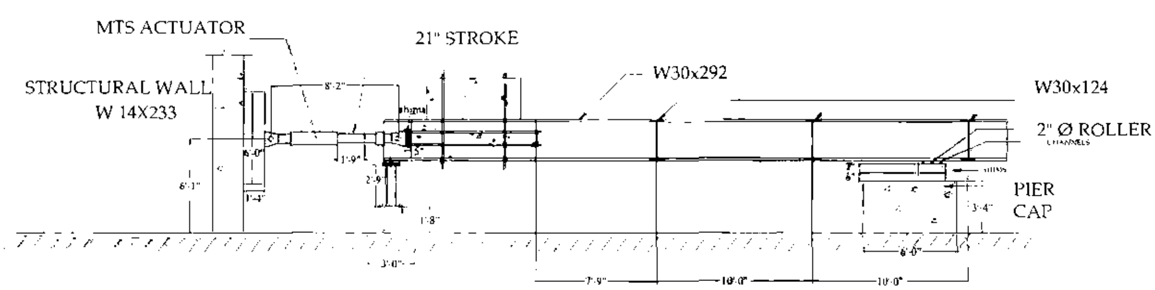

Figure A2: Experimental test setup of 40' bridge specimen rehabilitated with tall-33½" pedestals

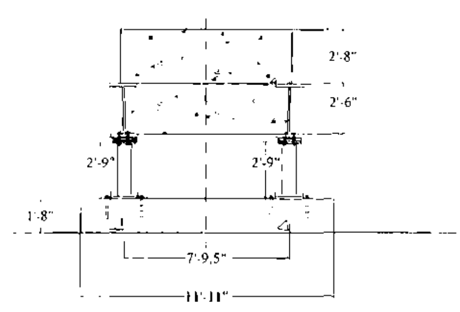

Figure A3: Cross-section of experimental test setup with tall-33½" pedestals

A2. Evaluation of the performance of bridge steel pedestals

A2.1 Pedestal orientations and connectivity tested

In various GDOT bridge plans, different orientations and connectivity were noted. Therefore, six full-scale experimental tests were conducted on short-19" and tall-33½" steel pedestals to study and evaluate the performance of these orientations and connectivity of the anchor bolts on the global response. The tests were conducted in three phases, where the short-19" pedestals were tested in Phase I and the tall-33½" pedestals were tested in Phases II and III. All post-installed stud anchor bolts used for the experimental testing consisted of stainless steel and are 1¼" in diameter, 16" in length, and embedded 12" into the reinforced concrete pier. Table A1 shows a testing matrix of the pedestal orientation and post-installed stud anchor bolt connectivity for all tests. The dimensions for the base plate of each steel pedestal is noted along with the direction of loading from the hydraulic actuator that loaded the 40' bridge specimen at a rate of 2 inches per minute in displacement control.

Table A1: Testing matrix of pedestal orientation and connectivity

PHASE	SHORT-19" PEDESTALS			
P1-1	strong-axis (bolts through welded angles)	P	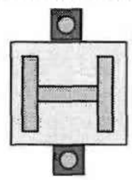	9" 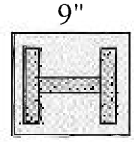 13"
P1-2	weak-axis (bolts through welded angles)	P	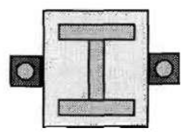	13" 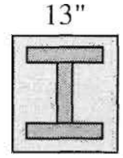 9"
PHASE	**TALL-33½" PEDESTALS**			
P2-1	strong-axis (bolts through welded angles)	P	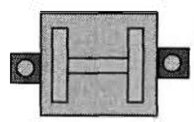	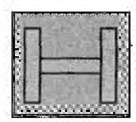 8" 19"
P2-2	strong-axis (bolts within cross-section)	P	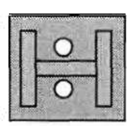	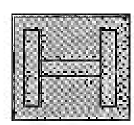 8"
P3-1	weak-axis (bolts through welded angles)	P	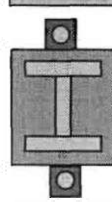	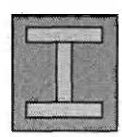 19" 8"
P3-2	weak-axis (bolts within cross-section)	P	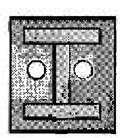	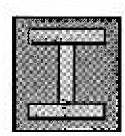 19"

A2.2 General observations

From the experimental testing, the steel pedestals remain elastic and are quite flexible members that undergo kinematic motion during cyclic loading, where both sliding and rocking occur. As a result of sliding on the ⅛" elastomeric (neoprene) pad, the steel pedestals are efficient in dissipating energy, which is very advantageous during earthquakes. From test results, the equivalent viscous damping of the steel pedestal compares favorably to traditional energy dissipating devices with damping ratios ranging from 5-22%, depending on the loading cycle. At the peak displacements, the damping ratios range from 8-17%. Table A2 shows the equivalent viscous damping computed at each target displacement for the six tests.

Table A2: Equivalent viscous damping ratios (%) for all six tests

Displacement	P1-1	P1-2	P2-1	P2-2	P3-1	P3-2
0.5	22.4	14.8	9.5	6.0	7.8	4.6
0.75	21.4	16.7		8.2	7.6	5.7
0.8			7.4			
1.0	15.3	16.6		4.7	6.9	13.2
1.4			7.9			
1.5	4.9	13.1		7.6	10.3	11.1
1.75	11.9					12.4
2.0		12.7		7.5	14.4	16.9
2.5		10.3		11.4		
2.75		11.8		6.9		
3.0		11.9		10.6		
3.25		12.6				
3.5				8.1		

Phase I (P1) of the tests compared the peak strength and deformation capacities between the 19" (short) pedestals, where loading was applied in the direction of its strong-axis (test P1-1) and weak-axis (test P1-2). The placement of the welded angles, for which the post-installed stud anchor bolts were connected, was based on the contractor's pedestal plans for GDOT Bridge No. 72. The orientation of loading along the short pedestals innately positioned the post-installed stud anchor bolts to be perpendicular to the plane of loading (but outside of the cross-section) for P1-1and in-plane of loading (but outside the cross-section) for P1-2. Note the similarity of the test setup for test P1-1 to an as-built photo of an existing (yet skewed) bridge in Georgia that has been rehabilitated with steel pedestals shown in Figure A4. (The effects of skew were beyond the scope of this project).

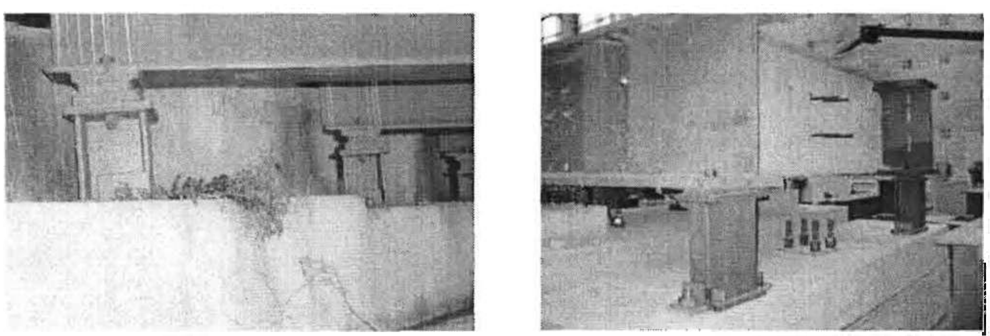

Figure A4: As-built photo of bridge with steel pedestals compared to experimental test setup (P1-1)

Phase II (P2) of testing consisted of loading the 33½" (tall) pedestals along its strong-axis of the built-up section but with two (2) different schematics for the location of the post-installed stud anchor bolts. The first bolt orientation, test P2-1, had L-shaped angles welded to the bottom plate of the pedestals similar to Phase I of testing. The second bolt configuration consisted of aligning the post-installed stud anchor bolts within the cross-section of the pedestal. The second configuration was based on an existing placement of bolts on the George W. Thompson Sr. Memorial Bridge on Thornton Road (Austell, Georgia) that crosses over I-20 West. Note the similarity in the test setup for test P2-2 and the as-built photo shown in Figure A5.

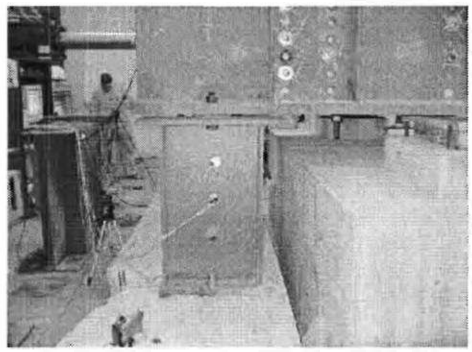

Figure A5: As-built photo of bridge with steel pedestals compared to experimental test setup (P2-2)

The setup for Phase III (P3) was similar to Phase II (P2) in that the 33½" (tall) pedestals were used but now loaded in the direction of its weak-axis of bending. Additionally, the intermediate plate was removed as quite a bit of slip was observed in previous tests as a result of poor contact between surfaces. Kinematic relationships from the displacement results measured by the instrumentation showed slip up to 0.3" at the interface between the girders and pedestals. The intermediate plates were removed to provide stiffer connectivity between the girders and pedestals. One advantage of having the intermediate plates is that it provides separation between the underside of the girders and the top plate of the steel pedestals, thereby allowing more opportunity for the pedestals to undergo larger angles of rotations as the pedestals rock as observed in test P2-2 and Figure A6.

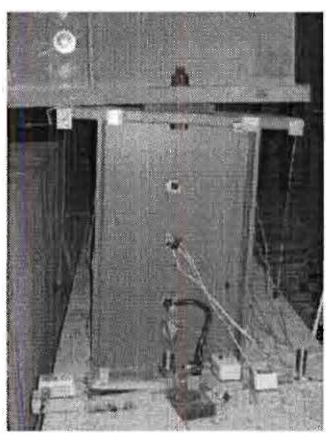

Figure A6: Test P2-2 exhibited the largest peak displacement of 3.5" and angles of rotation (rocking)

A2.3 Force-displacement relationships

Six (6) force-displacement relationships of the hysteretic behavior were obtained. The hysteretic behavior from the force-displacement relationships showed the inherent ability for the steel pedestals to dissipate energy through a phenomenon of sliding and rocking. For instance, the pedestals would slide on the ⅛" elastomeric pad and then rock, bearing on one edge of the pedestal bottom plate and prying the anchor bolts within the reinforced concrete pier on the side where uplift was observed.

Comparing tests P1-1 and P1-2 (Figure A7), test P1-2 consisting of the 19" (short) pedestals loaded along its weak-axis was able to resist the larger peak maximum and minimum loads before a mechanism leading to a mode of failure occurred (details discussed in next section of this report). Almost 1" of sliding occurs. The remainder or "pinching" of the hysteresis shows the rocking experienced by the pedestals. This region is smaller in that more energy is dissipated as the pedestals undergo sliding. In fact, from all of the test data collected, test P1-2 exhibited the largest peak maximum and minimum loads at -96.35 kips (compression) and 78.15 kips (tension). Test P1-2 also exhibited the second largest peak maximum and minimum displacements of 3.25" and -3.25", respectively, just shy of ±3.5" exhibited in test P2-2. One reason for test P1-2 (short, weak-axis) to show larger forces and displacements can be attributed to the smaller moment of inertia, enabling the pedestal to be less stiff (more flexible).

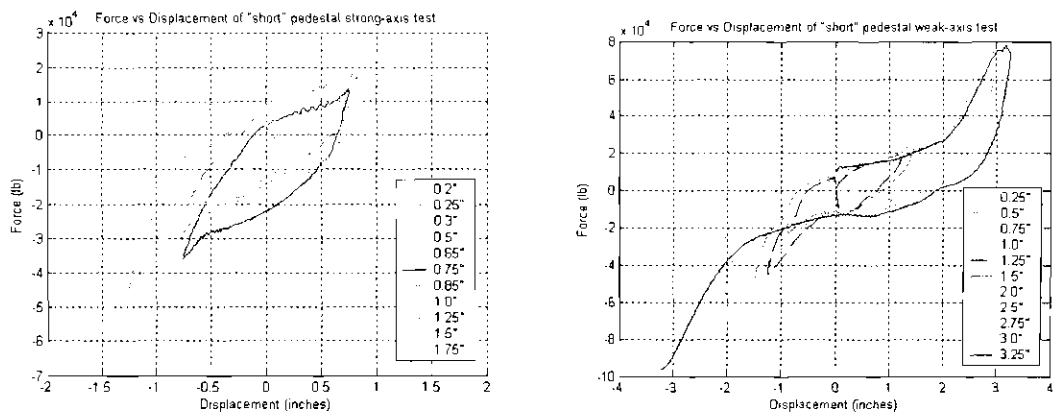

Figure A7: Force-displacement hysteretic behavior for tests P1-1 and P1-2

Test P2-1 exhibited the smallest peak loads and displacements due to fracture of the weld being in flexure as the pedestals rocked, thereby bearing on the weld. Once the welds fractured, connectivity between the anchor bolts and pedestals was lost. The dead weight of the prevented the tall pedestals from becoming unstable in this quasi-static environment. However, given a dynamic event such as an earthquake, the potential for instability is not eliminated. It is important to note that the size contrast between the base plate of the tall pedestals (Phase II and III) to the base plate of the short pedestals (P1). The relatively smaller base plate of the tall pedestals results shorter moment arms employed to resist the moments in the system. Test P2-2 was able to reach peak maximum and minimum displacements of ±3.5" before a concrete blowout mechanism occurred. Having the anchor bolts within the cross-section also enabled the pedestals to be more flexible in that the anchor bolts were positioned along one of the centroidal axes and close to the pedestal's center of rigidity as shown in Figure A8. Test P2-2 reached the largest peak displacement of 3.5" for all six tests conducted.

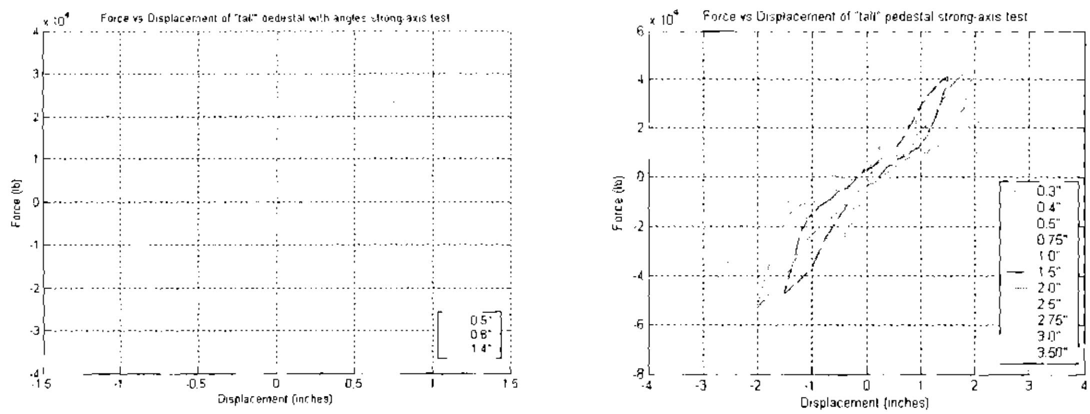

Figure A8: Force-displacement hysteretic behavior for tests P2-1 and P2-2

In terms of loads from Phase III, test P3-2 was able to resist slightly larger loads in compression than test P3-1. However, testing was stopped due to resonance experienced by the servovalve in the hydraulic actuator. If testing were continued, gradual stiffness degradation along a similar slope already observed would have continued as prying action of the post-installed stud anchor bolts was observed. The minor technical difficulty experienced did not affect the results; the hysteretic behavior of the tall pedestals tested along its weak-axis is adequately captured for use in an appropriate analysis of the tall pedestal orientations and connectivity tested in Phase III (Figure A9).

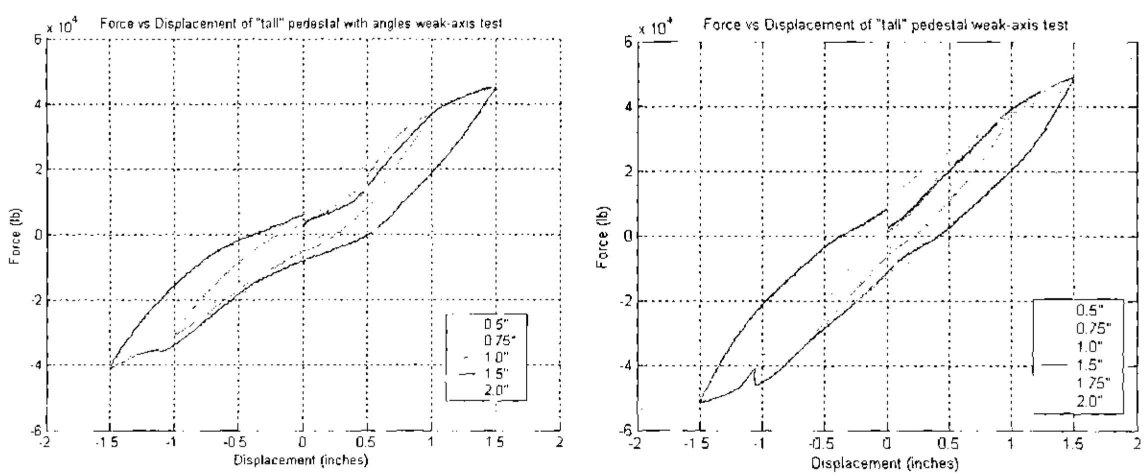

Figure A9: Force-displacement hysteretic behavior for tests P3-1 and P3-2

A3. Mechanisms leading to modes of failure of post-installed stud anchor bolts

Experimental test results indicated three major mechanisms that can lead to modes of failure for a 40' bridge simply-supported bridge span rehabilitated with steel pedestals: i) prying-action of post-installed stud anchor bolts (predominant mode), ii) bolts yielding, and iii) concrete breakout (or concrete edge failure). All three of these mechanisms are anticipated failure modes of anchors under shear loading as reported by the American Concrete Institute (ACI) Committee 318 (Appendix D)[1] and Eligehausen, Mallee, and Silva (2006).[2] Weld fracture was observed in test P2-1, resulting in two of the three mechanisms leading to modes of failure (bolts yielding and concrete breakout). This configuration where the pedestals are relying heavily on the welds subjected to flexure from the cyclic loading can be problematic in the event of an earthquake. Details of all the mechanisms leading to modes of failure for the post-installed stud anchor bolts for steel pedestals are described in this section.

A3.1 Prying-action

Prying-action of the post-installed stud anchor bolts was the predominant mechanism observed in all of the tests, leading to surface failures (concrete breakout) or yielding of the bolts in certain cases. Prying-action causes spalling or crushing of the surrounding concrete, thereby inducing bearing stresses in the concrete (Figure A10). As the surface concrete spalls or crushes, there is a shift of the centroid of resistance of the concrete breakout shear strength. It was observed that with increasing loads, the stud elongates and the baseplate rotates and loses contact with the concrete surface. As a result, a compression force between the baseplate and concrete as well as a tensile force in the stud anchor bolt generate a moment. These forces can be translated into how the stud anchor bolt performs as a load-bearing mechanism.[2]

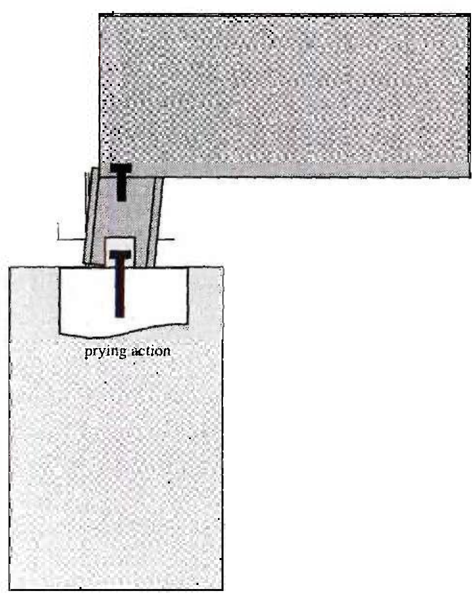

Figure A10: Prying-action of stud anchor bolts causing spalling or crushing of surrounding concrete

[1] *Building Code Requirements for Structural Concrete (ACI 318-02) and Commentary (ACI 318R-02).*

[2] Eligehausen, R., Mallee, R., and Silva, J. *Anchorage in Concrete Construction*, Ernst & Sohn, Berlin, 2006.

The tests with the most pronounced prying-action are presented and their performance is evaluated. Table A3 shows the peak displacements and peak loads for each test, where the peak is defined when a mechanism leading to a mode of failure occurred and the test was stopped. The layout of the bolts was strategically placed to particularly evaluate the performance of concrete edge distance, especially since close edge distances were observed in the field (Figure A5). Pictured below are the failure surfaces from tests P1-1 and P1-2 of the reinforced concrete pier subjected to shear loading close to an edge (Figures A11 and A12). The diagonal crack propagated through the depth of the 20" reinforced concrete pier as shown in Figure A12. Should the testing have continued, the concrete breakout strength would have been exceeded. Tests revealed a failure surface angle of approximately 35° as referenced in ACI 318-02, Appendix D. This provides validation to the testing and raises concern to addressing minimum concrete edge distances for the stud anchor bolts of steel pedestals, which will be discussed in the *Recommendations for Steel Pedestals* noted later in this report. Figure A13 shows slip of the nut on the stud anchor bolt as a result of the engaging the anchor bolt as the pedestal rocks in test P2-2, which was a phenomenon commonly observed in all of the tests.

Table A3: Peak displacements and loads for all six reversed cyclic, quasi-static tests

Test Description	Peak displacement (inches)	Peak tensile/compressive loads (kips)
P1-1	±1.75	25/-65
P1-2	±3.25	78/-96
P2-1	±1.4	36/-30
P2-2	±3.5	54/-60
P3-1	±2.0	53/-46
P3-2	±2.0	55/-53

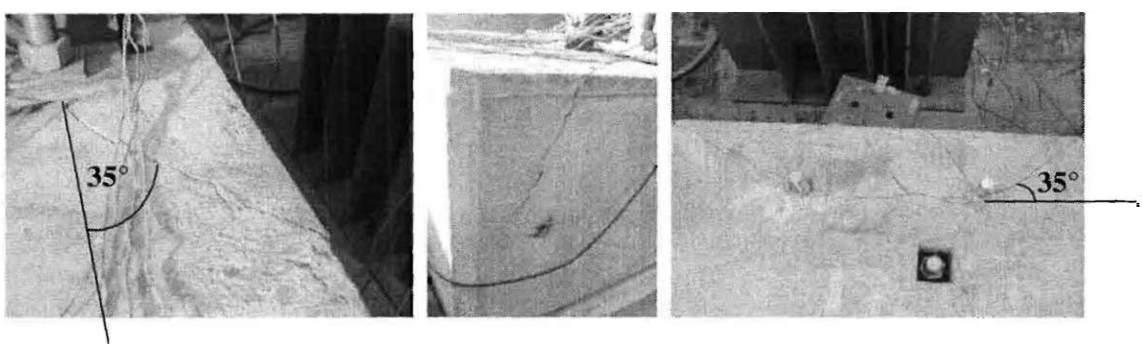

Figure A11: Failure surface with diagonal crack of 35° revealing concrete breakout strength

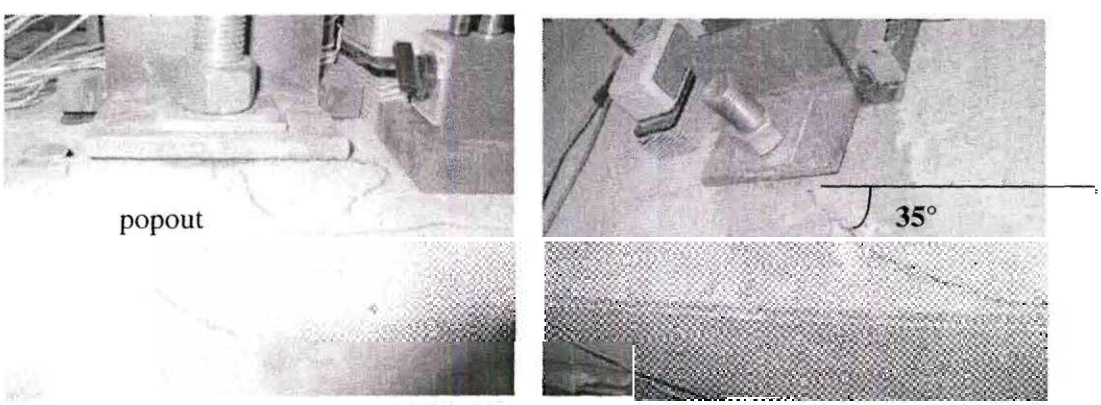

Figure A12: Failure surface with diagonal crack of 35° revealing concrete breakout strength

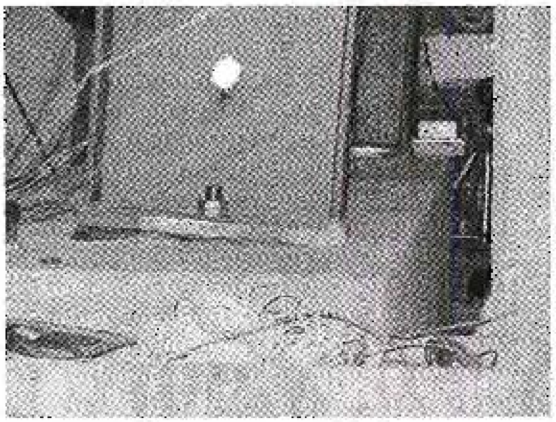

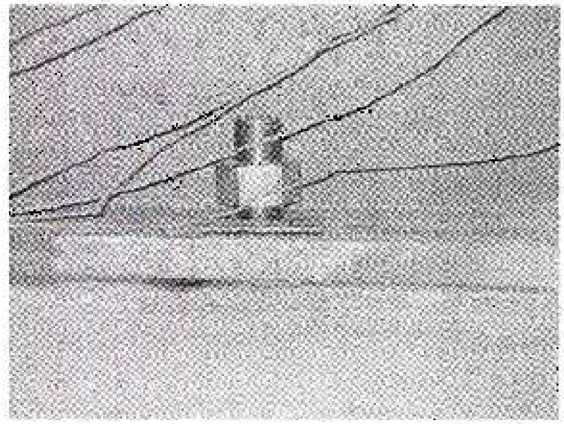

Figure A13: Slip of nut on stud anchor bolt as a result of prying-action as the pedestals rocked

A3.2 Bolts yielding

The second mechanism observed was yielding of the post-installed stud anchor bolts. Yielding occurred at relatively large displacements and loads. Figure A14 shows a schematic of yielding of the bolts and the actual yielding observed in test P1-2, where peak loads were 78 kips (tensile loading) and -96 kips (compressive loading) and peak displacements were 3.25". Sufficient resistance was provided by the anchor bolts in that there was adequate embedment length of the bolts into the concrete pier and adequate concrete edge distance such that concrete breakout did not occur. Consequently, yielding of the bolts allowed for greater strength and deformation capacity within test P1-2, where ductility of the anchor bolts was engaged. Having the bolts to yield indicates that there is adequate embedment depth and minimum edge distance to assure failure in the bolts and not the concrete pier. Additional factors that can affect the mechanism that leads to a mode of failure is the anchor bolt strength, diameter of anchor bolt, concrete strength and anchor bolt spacing. Mechanical dial gauges were connected to measure uplift (pullout) of the bolts. For all of the tests, the maximum pullout was 0.2". Testing was stopped at the onset of noticing yielding of the bolts such that a catastrophic failure did not result with continued loading.

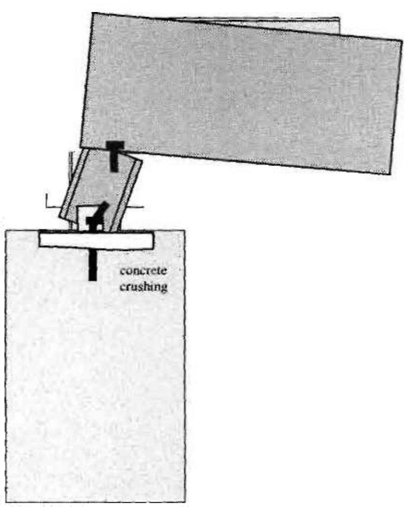

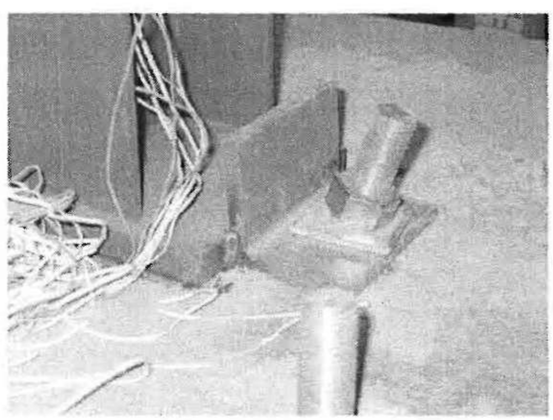

Figure A14: Schematic (left) and photo of bolts yielding (right) in test P1-2

A3.3 Concrete breakout

The third mechanism that can lead to a mode of failure is concrete breakout, also called concrete edge failure. Concrete breakout occurs when the concrete fractures before the load-carrying capacity of the steel is reached. Figure A15 shows a side-view schematic of the surface failure, where the surface failure on top of the concrete pier occurs at an angle of 35° (Figure A16, right). For test P2-1, the tall pedestal was loaded along the plane of the strong-axis of the steel pedestal. The angle was welded to the base plate in the direction of loading such that the weld that connects that angle to the pedestal base plate was in flexure during cyclic loading. Weld fracture occurred as welds are typically weak in flexure. The fracture disengaged the anchor bolt to the pedestal. However, due to sliding of the pedestal, the base plate of the pedestal reconnected to the weld and reactivated the resistance of the anchor bolt based on frictional contact alone. When the load in the system exceeded the allowable resistance provided by frictional contact with the weld, concrete breakout resulted and testing was stopped. The concrete breakout essentially consisted of unconfined concrete as a result of the anchor bolt being close to the edge of the concrete pier. The surface failure occurred at the predicted angle of 35° for test P2-1. Since limited resistance was provided by this anchor bolt configuration and connectivity, the peak displacement was 1.4" and peak tensile and compressive loads were 36 kips and -30 kips, respectively, for test P2-1.

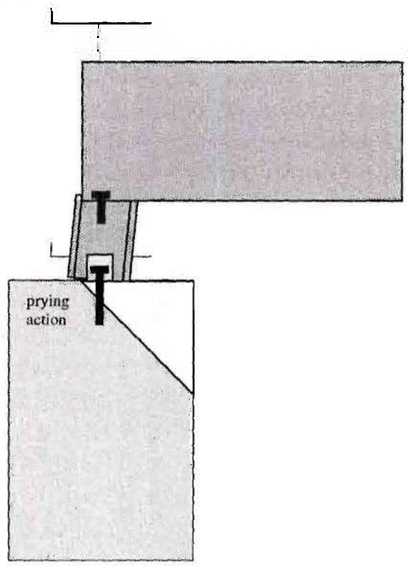

Figure A15: Side-view schematic of concrete breakout for anchors close to the edge of the concrete pier

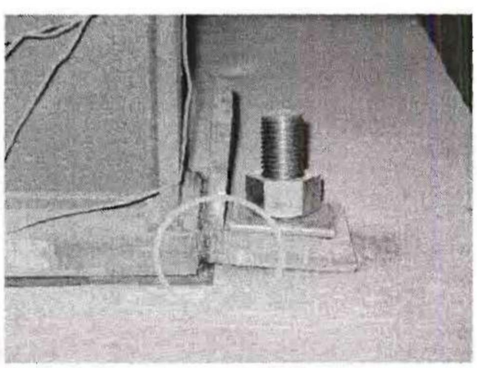

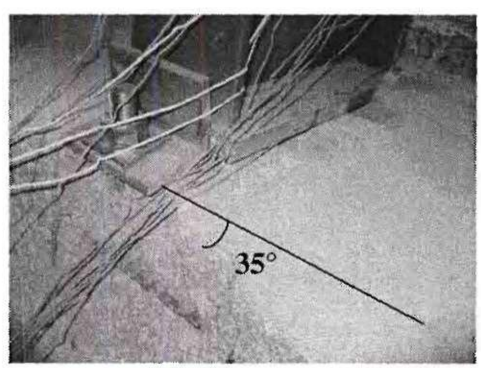

Figure A16: Onset of weld fracture of angle (left) and concrete breakout at 35° on concrete pier (right)

B. ANALYSES OF BRIDGE STEEL PEDESTALS

B1. Uniform Hazard Spectra for Three Cities in Georgia

Using the *Probabilistic Hazard 3.10* software[5] produced by Frankel, A. D. and Leyendecker, E. V., uniform hazard spectra are generated for Atlanta, Cartersville, and Ringgold, Georgia given a 500, 1000 and 2500-year return period earthquake. The uniform hazard spectra (UHS) are determined based on a probabilistic seismic hazard analysis that considers site conditions, bin sizes, and probability of exceedance (% PE) for an event in the specified area. The spectra show the spectral acceleration in units of g versus the given periods in units of seconds for 5% damping, for the range of periods that can be expected for the pedestrals that were tested. Note that these results are conservative since the pedestals revealed 5-22% damping ratios as shown in Table A2. Figures A17-A19 show the expected spectral accelerations for Atlanta (Fulton County), Cartersville (Bartow County), and Ringgold (Catoosa County), Georgia given a 500, 1000 and 2500-year return period earthquake.

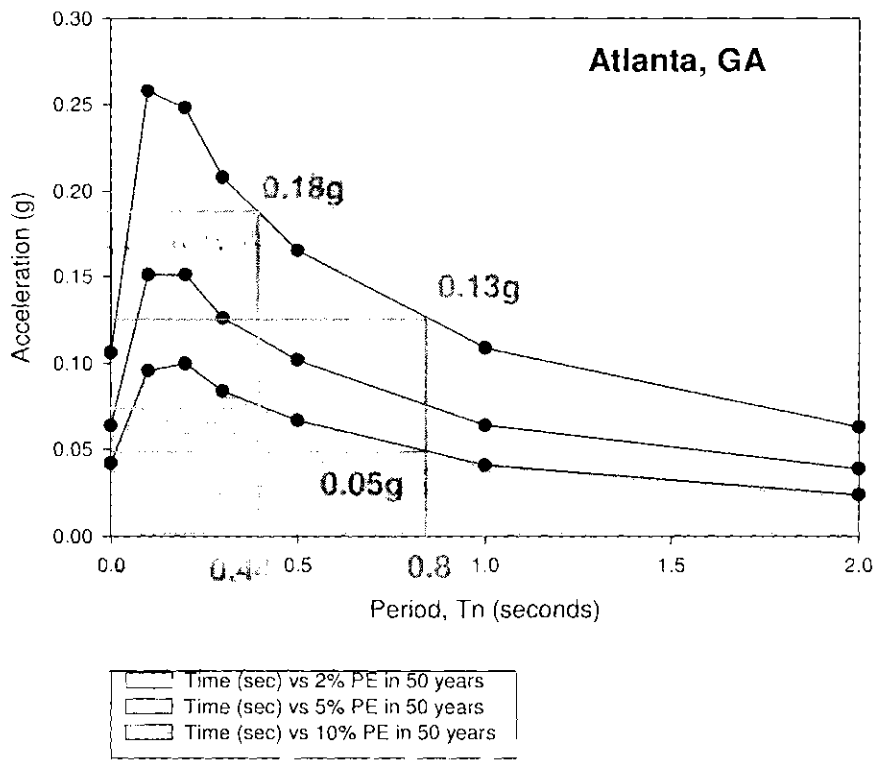

Figure A17: Uniform hazard spectra for Atlanta, GA for 2500, 1000, and 500-year return period EQ

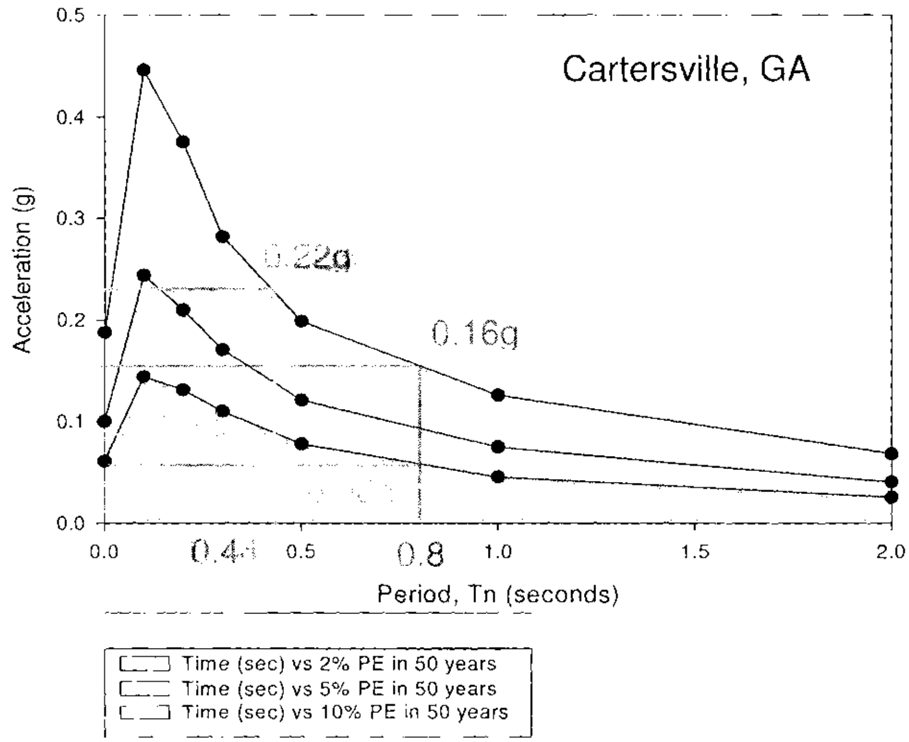

Figure A18: Uniform hazard spectra for Cartersville, GA for 2500, 1000, and 500-year return period EQ

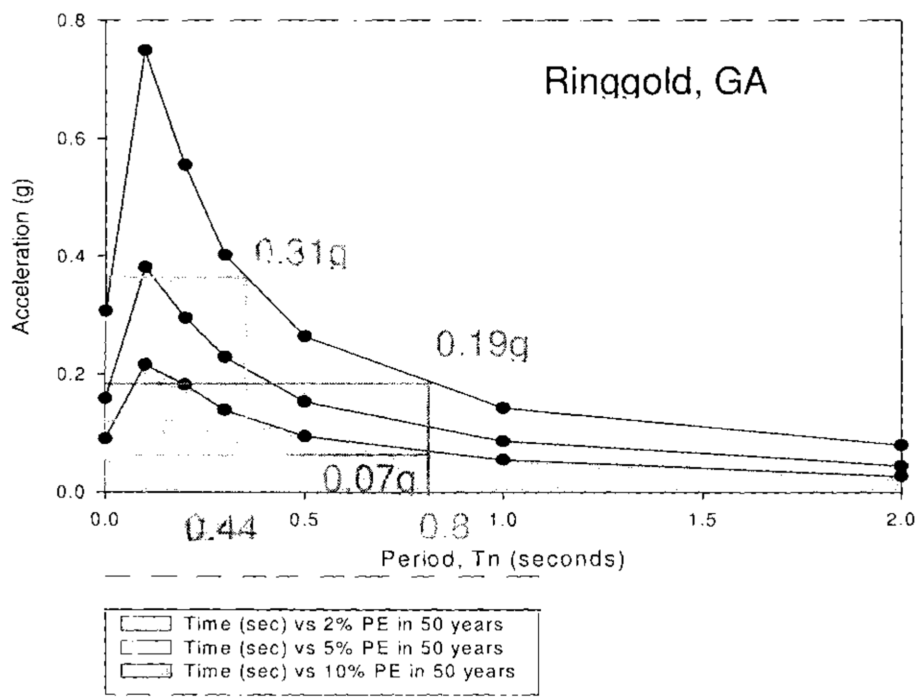

Figure A19: Uniform hazard spectra for Ringgold, GA for 2500, 1000, and 500-year return period EQ

B2. Example problem for bridge vulnerability assessment

An example problem is provided for bridge vulnerability assessment based on a 10-step procedure outlined in Section D of the *Recommendations for Bridge Steel Pedestals.*

Problem Description:

A multi-span, simply-supported composite-action bridge having 6-spans and a length of 410' has been rehabilitated with 19" steel pedestals oriented similar to test P1-1 conducted at the Georgia Institute of Technology[3]. At Abutments 1 and 2, there is a single row of 3 pedestals, but 6 pedestals (front and back) at the other bents giving a total of 36 pedestals. The bridge is located in Atlanta, Georgia, and needs to be assessed for seismic vulnerability.

Properties:

- The total bridge mass, including the pedestals, columns and deck, is 5 k-s^2/in.
- The bridge deck has a depth of 7" where there is composite action with the girders.
- The square columns and rectangular bents provide a total length of 15'. All columns have equal heights. A total clearance of 17' is provided from the installation of the 19" steel pedestals.

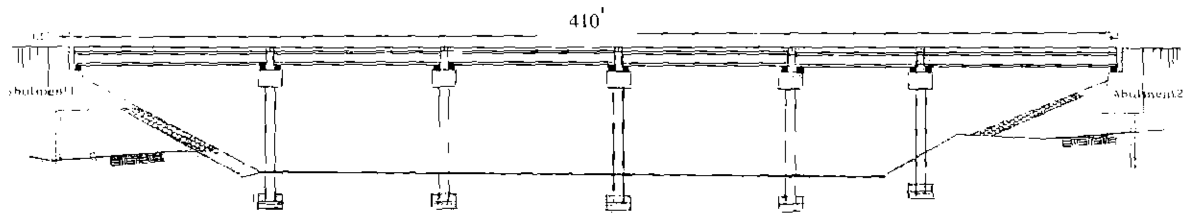

STEP

1. The total mass, M, is 5 k-s^2/in and the summation of stiffness from all of the columns, $K_{columns}$, is 6,538 k/in.

2. There are a total of 36 pedestals. The bridge in this example is rehabilitated with 19" steel pedestals that are loaded along its strong-axis similar to test P1-1 noted in Table A4.

TableA4: Initial and peak effective stiffness values from force-displacement hysteretic relationships

Test	Initial Effective Stiffness of a Pedestal	Peak Effective Stiffness of a Pedestal
P1-1	***18.6***	***13.4***
P1-2	17.9	13.5
P2-1	20.5	12.1
P2-2	27.1	8.27
P3-1	20.4	24.8
P3-2	24.8	13.7

[3] Hite, M., DesRoches, R., and Leon, R., Georgia Institute of Technology, GDOT RP2048, 2004-06.

3. The initial and peak effective stiffness is 18.6 and 13.4, respectively. Multiplying each stiffness by 36 pedestals yields the combined initial and peak effective stiffness, $K_{pedestals}$, to be 668.7 and 482.4 k/in, respectively. Typically, the pedestal stiffness is more flexible than the stiffness of the columns, therefore controlling Equation 1 presented in Step 4.

4. The range of total stiffness is 477 to 660 k/in, applying Equation 1.

$$\sum K = \frac{K_{pedestals} K_{columns}}{K_{pedestals} + K_{columns}} \qquad \text{Eq. 1}$$

5. Using Equation 2, the natural frequency and structural can be determined by T_n = 0.53 to 0.63 seconds.

$$\omega_n = \frac{2\pi}{T_n} \quad \text{and} \quad T_n = 2\pi\sqrt{\frac{m}{\sum K}} \qquad \text{Eq. 2}$$

6. The uniform hazard spectra is shown below:

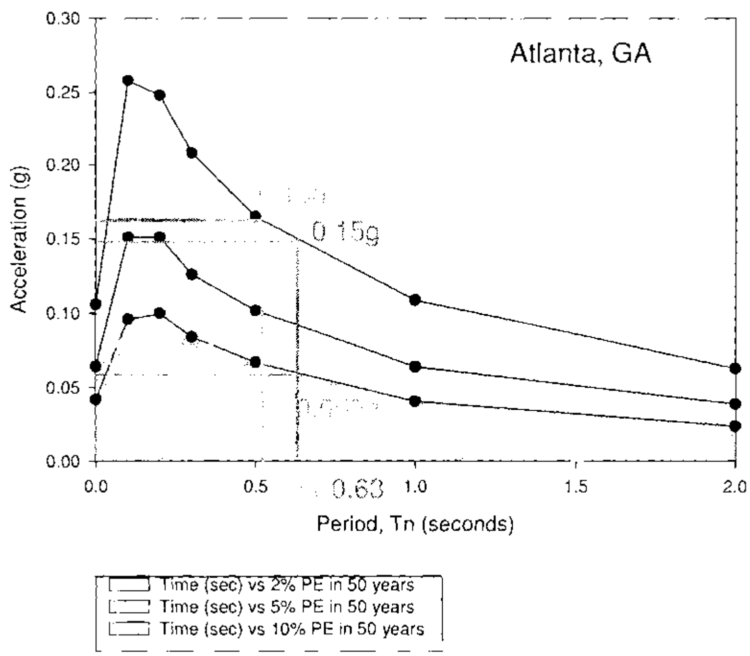

7. The maximum spectral accelerations for the structural period range of 0.53 seconds to 0.63 seconds correspond to 0.16g and 0.15g for the 2500-year return period earthquakes.

8. The displacements are calculated using Equation 3 and are shown in Table A5 as the displacement demand (units = inches).

9. The demand-to-capacity (D/C) ratios are shown in Tables A5. The displacement demand is divided by the peak displacement of 1.75" (capacity) obtained from test P1-1.

10. All ratios are "safe" as they are less than 1. However, larger displacements can be associated with the higher structural period of 0.63 seconds. The more vulnerable case for this example is highlighted, where less than 1 inch of structural displacement can be anticipated for the 2500-year return period earthquake. The D/C ratio can be used for bridge vulnerability assessment and prioritization for maintenance and inspection of bridges. If the D/C ratio for this example was not declared "safe," then different pedestals and orientations that correspond to the appropriate stiffness shall be considered such that the D/C ratio is less than 1. Further studies and re-design may also be required for these cases.

Table A5: D/C ratio for short-19" steel pedestals loaded along its strong-axis (P1-1, 1.75" capacity)

% PE in [illegible]	Demand [illegible]	[illegible]
2% Tn=0.53s	0.44"	**0.25**
5% Tn=0.53s	0.27"	**0.15**
10% Tn=0.53s	0.18"	**0.1**
2% Tn=0.63s	[illegible]	**0.33**
5% Tn=0.63s	0.36"	**0.23**
10% Tn=0.63s	0.23"	**0.13**